Iranian Journal of Science (2024) 48:213–227
https://doi.org/10.1007/s40995-023-01564-x

RESEARCH PAPER

Casing Reliability Evaluation of HTHP Wells Via Uncertainty and Stress–Strength Interference Theories

Chao Han[1,2] · Rongdong Dai[1] · Wenxue Pu[3] · Zhichuan Guan[4] · QiZhong Tian[1] · Haibin Zhao[3] · Xianming Ma[4] · Shengnan (Nancy) Chen[5] · Bo Zhang[6] · Chenglong Li[1,2] · Hui Shao[3] · Cong Zhang[3]

Received: 2 September 2023 / Accepted: 19 November 2023 / Published online: 8 January 2024

Abstract

Casing reliability is essential for the high-temperature high-pressure (HTHP) wells. The complicated downhole geological environment, high casing external load during the drilling stage, and annulus pressure in the production stage may all lead to casing collapse and wellbore integrity failure. Thus, it remains a hot topic to quantitatively evaluate the casing reliability throughout the whole life cycle (WLC) of HTHP wells. In this paper, a WLC quantitative evaluation method of casing reliability of HTHP wells in the whole borehole section is established based on the Monte Carlo simulation and the stress–strength interference theory. More specifically, WLC casing load is calculated by integrating the annulus pressure, casing load under non-uniform in situ stress, and the drilling extreme conditions. The casing strength calculation model of HTHP wells is then established by the K-T formula, while considering the temperature effect on casing strength to compute the casing reliability. The proposed method is applied in an HTHP gas well in the South China Sea. The results indicate that, under the hollowing degrees with allowable safety factors, there is still some risk in the casing running and lost circulation conditions. The failure risk at the weak points of each spud is within 0.08–0.2 in the casing running condition and within 0.1–0.5 in the lost circulation condition. For the production stage, before and after annulus pressurization, the overall trend of the casing safety factor of anti-internal-pressure remains the same and decreases with increasing well depth. The weak points exist at the inner cement surface or boundary point of different wall thickness casings. The risk of casing extrusion after annulus pressurization increases with decreasing well depth. Due to the lack of consideration of annulus pressure and uncertainty in the conventional casing-strength design methods, there is a possible failure risk at the casing weak points after annulus pressurization, where the reliability at the weak points on both side casings of annulus C is within 0.55–0.67 under annulus pressure 19MPa. The research verifies that the casing strength design should leave a margin in the HTHP environment to avoid high temperatures reducing reliability. Under the leak-prone strata condition, the casing strength at weak points should be strengthened accordingly. The casing-strength design considering annulus pressure and uncertainty will improve the casing reliability. In addition, this method can also be used to calculate the maximum allowable annulus pressure and the maximum allowable hollowing degree under the existing production and drilling plans, thus helping to optimize production and casing strength design.

Keywords HTHP wells · Casing reliability · Annulus pressure · Stress–strength interference theory · Hollowing degree · Uncertainty theory

1 Introduction

High-temperature high-pressure (HTHP) wells are becoming routine practice nowadays, especially in deep-water (Jaimes et al. 2022; Seymour and MacAndrew 1993) or deep-stratum (Liu et al. 2019; Cao et al. 2022) blocks. The HTHP well casings are located in a complex downhole environment with problems such as HTHP, large in situ stress, strong uncertainty of formation pressure, and narrow safety pressure window (Guan et al., 2018; Ming et al. 2019; Zhong 2016). In addition, complex situations such as lost circulation (Shen 2015; Xie et al. 2021) and gas kick (Gu et al. 2021; Yin et al. 2022) during the drilling process can easily lead to casing hollowing and deformation

Extended author information available on the last page of the article

damage at the casing shoe. Moreover, high annulus pressure will be generated during the production stage due to the change of temperature field (Oudeman and Kerem 2006), corrosion and leakage of pipes (Zhang et al. 2021; Zhang et al. 2020), and sealing failure of cement sheath (Jin et al. 2013). Thus, huge challenges are encountered to maintain the wellbore integrity for HTHP wells. Recent researches on the reliability of HTHP well casing mainly focus on the annulus pressure (Dong and Chen 2017), calculation of casing load and strength (Guohua et al. 2012; Wang et al. 2015; Zhao et al. 2021), and evaluation methods (Li et al. 2021; Muoghalu et al. 2020; Wang et al. 2020). The principle and calculation models of annulus pressure have been preliminarily verified. It can be divided into trapped annulus pressure and sustained annulus pressure according to different origins. The trapped annulus pressure generally exists in the sealed annulus of the HTHP well, which is caused by the different expansion coefficients of the casing and annulus fluid. Scholars in the industry mainly research the calculation method of trapped annulus pressure from the aspects of PVT properties of the fluid (Oudeman and Kerem 2006), wellbore structure (Bo et al. 2015), and temperature–pressure coupling (Bailing et al. 2015). The sustained annulus pressure is mainly caused by the formation-fluid crossflow caused by wellbore integrity failure. The calculation model of sustained annulus pressure can be established based on the principles of gas mass conservation and annulus volume conservation (Zhang et al. 2018; Zhang et al., 2022). In addition, the sustained annulus pressure can be prevented by optimizing the ductile micro-expansion cement slurry and using the isolated liner hanger (Yang et al. 2018). For the calculation of casing load, the analytical solution of casing-cement sheath-stratum system stress distribution is obtained mainly through numerical simulation and mechanical derivation, considering non-uniform in situ stress and thermal-solid coupling (Qian and Gao 2011; Yin et al. 2006). At present, the latest casing strength calculation method in the industry is the K-T formula. Previous research shows that the influence of temperature on casing strength under the HTHP environment is mainly reflected in the change of pipe yield strength and elastic modulus (Wenkui et al. 1900). The traditional safety factor method is mainly used in the field to evaluate the reliability of casing. In recent years, domestic and foreign scholars have successively established evaluation methods based on the theories of stress–strength interference (Liao et al. 2012), neural network (Wang et al. 2020), reliability (Li et al. 2021; Zhu and Liu 2018) and Monte Carlo simulation (Muoghalu et al. 2020). For wells containing sour gas, the life of the casing is predicted considering the influence of steel corrosion on the residual strength of the casing (Kuanhai et al. 2022; LIAN et al. 2018). Through preliminary research, it can be found that the current evaluation of casing reliability mainly focuses on the case where the annulus is not pressurized after cementing, and the strength check of pressurized annulus casing mainly focuses on the local check with defects in the case of corrosive gas. The overall variation rule and dangerous points of casing reliability after annulus pressurization are still unclear, and there is a lack of reliability analysis of casing under different hollowing degrees in case of downhole risks such as lost circulation and gas kick during drilling.

In this paper, casing strength and load under the annulus pressure and extreme conditions during drilling are investigated based on the uncertainty analysis method and stress–strength interference theory. A WLC quantitative risk evaluation method for the whole borehole section of HTHP well casing is established considering the temperature effect on casing strength and load. This study provides a theoretical foundation and technical support for the reliability evaluation and optimal design of HTHP well casing in deep-water and deep-stratum formations.

2 Methodology

As shown in Fig. 1, the methodology can be divided into three sections. The first section is the WLC calculation model of casing load. The main consideration in the production stage is the effect of annulus pressure and non-uniform in situ stress. And the well construction stage mainly considers the extreme conditions with hollowing or ultimate pressure inside the casing, including casing running, lost circulation, gas kick, cementing, and casing-pressure-testing.

The second section is the calculation model of casing strength. The last section is the quantitative evaluation method of casing reliability, which is based on the calculation results of casing load and strength and considers the effect of the HTHP environment.

2.1 WLC Calculation Model of Casing Load

2.1.1 Well Construction Stage

In the casing running condition, the closed-up casing running technique is usually adopted. It can realize the purpose of increasing the buoyancy of casing and reducing the hook load by reducing the liquid level inside the casing and improving the hollowing degree. The casing is subject to effective external extrusion pressure, and the calculation formula is as follows:

$$p_{ce} = \begin{cases} 0.00981\rho_{max}h & h < H_s k_m \\ 0.00981\rho_{max}H_s k_m & h \geq H_s k_m \end{cases} \quad (1)$$

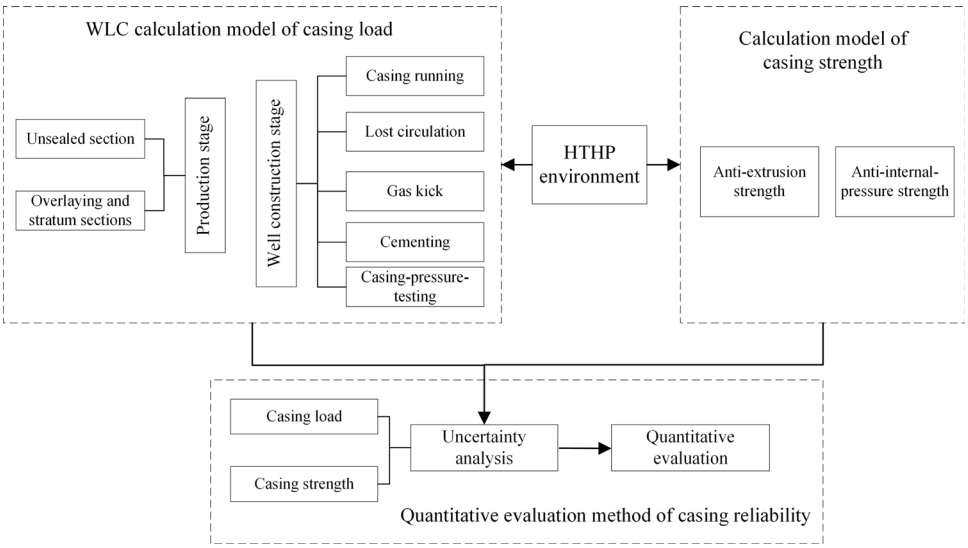

Fig. 1 Flow chart of WLC quantitative evaluation method of casing reliability of HTHP wells

where p_{ce} denotes the effective external extrusion pressure, MPa; k_m denotes the hollowing degree, dimensionless (that is, the ratio of the liquid level drop height in the casing from the wellhead to the casing shoe depth); ρ_{max} denotes the maximum drilling fluid density in the current spuds, g·cm^{-3}; H_s denotes the depth of casing shoe, m.

In the lost circulation condition, the most dangerous situation of the casing is considered, that is, lost circulation occurs at the beginning of the next spud. At this time, the density of drilling fluid in the wellbore is the minimum value for the next spud. Lost circulation causes a drop in liquid level in the wellbore, and the casing is subject to the effective external extrusion pressure, the calculation formula is as follows:

$$p_{ce}=\begin{cases}0.00981\rho_{max}h & h<H_{ce}\\ 0.00981[\rho_{max}H_{ce}+\rho_{ce}(h-H_{ce})] & H_{ce}\le h<H_sk_m\\ 0.00981[\rho_{max}H_{ce}+\rho_{ce}(h-H_{ce})-\rho_{nmin}(h-H_sk_m)] & h\ge H_sk_m\end{cases} \quad (2)$$

If $H_{ce}\ge H_sk_m$,

$$p_{ce}=\begin{cases}0.00981\rho_{max}h & h<H_sk_m\\ 0.00981[\rho_{max}H_sk_m+(\rho_{max}-\rho_{nmin})(h-H_sk_m)] & H_sk_m\le h<H_{ce}\\ 0.00981[\rho_{max}H_{ce}+\rho_{ce}(h-H_{ce})-\rho_{nmin}(h-H_sk_m)] & h\ge H_{ce}\end{cases} \quad (3)$$

If $H_{ce}<H_sk_m$,where H_{ce} denotes the depth of cement surface, m; ρ_{nmin} denotes the minimum drilling fluid density in the next spud, g·cm^{-3}; ρ_{ce} denotes the density of cementing slurry, g·cm^{-3}.

In the condition of gas kick, it is necessary to shut in and hold the pressure to balance the bottomhole pressure. Considering the most dangerous scenario for casing, the stratum at the casing shoe is fractured during well shut-in and pressure build-up. And the casing is subject to effective internal pressure. The calculation formula is as follows:

If $H_{ce}<H_sk_m$,

$$p_{be}=\begin{cases}P_f-0.00981(\rho_{nmin}H_sk_m+\rho_{max}h) & h<H_{ce}\\ P_f-0.00981[\rho_{nmin}H_sk_m+\rho_{max}H_{ce}+\rho_{ce}(h-H_{ce})] & H_{ce}\le h<H_sk_m\\ P_f-0.00981[\rho_{nmin}(H_s-h)+\rho_{max}H_{ce}+\rho_{ce}(h-H_{ce})] & h\ge H_sk_m\end{cases} \quad (4)$$

If $H_{ce}\ge H_sk_m$,

$$p_{be}=\begin{cases}P_f-0.00981(\rho_{nmin}H_sk_m+\rho_{max}h) & h<H_sk_m\\ P_f-0.00981[\rho_{nmin}(H_s-h)+\rho_{max}h] & H_sk_m\le h<H_{ce}\\ P_f-0.00981[\rho_{nmin}(H_s-h)+\rho_{max}H_{ce}+\rho_{ce}(h-H_{ce})] & h\ge H_{ce}\end{cases} \quad (5)$$

where P_f denotes the formation fracture pressure at casing shoe, MPa.

There is no hollowing in the cementing and casing-pressure-testing conditions, with cementing-bumping-pressure and casing-test-pressure in the casing. Under these conditions, the casing is subject to effective internal pressure, and the calculation formula is as follows:

$$p_{be} = \begin{cases} P_t + 0.00981h(\rho_m - \rho_{max}) & h < H_{ce} \\ P_t + 0.00981[h\rho_m - \rho_{max}H_{ce} - \rho_{ce}(h - H_{ce})] & h \geq H_{ce} \end{cases} \quad (6)$$

where ρ_m denotes the minimum drilling fluid density in the next spud, if the analyzed casing is production casing and in the last spud, ρ_m denotes the maximum drilling fluid density in the current spud, g·cm^{-3}.

2.1.2 Production Stage

The main difference in the failure mode of casing between HTHP wells and conventional wells lies in the impact of HTHP on the load, specifically manifested in the annulus pressure. Annulus pressure generally occurs in the production stage. The main causations for it are gas crossflow caused by wellbore sealing failure, or annulus liquid expansion caused by annulus temperature and pressure change under good sealing condition. For trapped annulus pressure, it depends on the average changes of temperature and volume of the annulus section. According to the volume compatibility principle and the PVT property of annulus fluid, the calculation formula can be established (The details of the calculation model can be found in (Bo et al. 2015) and Appendix A). The sustained annulus pressure, caused by the gas crossflow, needs to be calculated through the conservation theorem of gas mass and annulus volume. Besides, it is assumed that the gas migration in the cement sheath is a one-dimensional unstable seepage in a single medium (The details of the calculation model can be found in (Zhang et al. 2018; Zhang et al., 2022) and Appendix B).

As shown in Fig. 2, the casing is vertically segmented into the unsealed section, the overlaying section, and the stratum section. According to the type of casing section and the source of load, the casing load calculation model is established.

1. Unsealed section.

The casing in the unsealed section is mainly affected by the hydrostatic pressure and annulus pressure.

2. Overlaying and stratum sections.

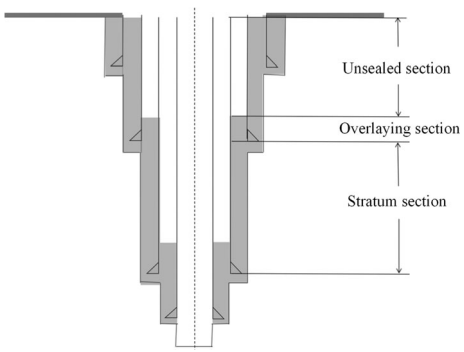

Fig. 2 Schematic diagram of casing section

The external extrusion pressure of the casing in the overlaying and stratum sections is derived from the in situ stress. Under the effect of in situ stress and annulus pressure, the casing in overlaying and stratum sections is subject to the same variation laws of the external extrusion pressure and Mises equivalent stress. Since the risk of casing failure in the overlaying section is smaller than that in the stratum section, to simplify the calculation, the overlaying section is considered as the stratum section for casing load calculation.

Based on elastic mechanics, the theoretical solution of the stress of casing-cement sheath-stratum system is established. The casing stress problem under non-uniform in situ stress can be decomposed into the stress problems under uniform in situ stress and deviating in situ stress (Yin et al. 2006), and the solutions of the two problems are obtained, respectively, for superposition.

The calculation formula of equivalent extrusion load under uniform in situ stress is as follows:

$$s_1 = (1 - v_s)(\sigma_H + \sigma_h) \left[1 + \frac{E_s(1 + v_c)}{E_c(1 + v_s)(1 - m^2)}(1 - 2v_c + m^2)\right]^{-1} \quad (7)$$

where σ_H, σ_h denote the maximum and minimum horizontal in situ stress, respectively, MPa; v_s, v_c denote the Poisson's ratio of stratum and casing, respectively, dimensionless; E_s, E_c denote the elastic modulus of stratum and casing, respectively, GPa; m denotes the ratio of inner diameter to the outer diameter of the casing, dimensionless.

Under the condition of deviating in situ stress, the calculation formula of extrusion load is as follows:

$$\begin{cases} s_2 = \dfrac{-2E_c(1 - v_s^2)(C_{22} + C_{12})}{E_s(1 + v_c)(C_{11}C_{22} - C_{12}C_{21})}(1 - m^2)^3(\sigma_H - \sigma_h) \\ s_3 = \dfrac{2E_c(1 - v_s^2)(C_{21} + C_{11})}{E_s(1 + v_c)(C_{11}C_{22} - C_{12}C_{21})}(1 - m^2)^3(\sigma_H - \sigma_h) \end{cases} \quad (8)$$

where C_{11}, C_{12}, C_{21}, C_{22} denote intermediate parameters obtained by simplifying stress distribution and displacement formulas of casing-cement sheath-stratum, respectively.

Finally, the equivalent external extrusion load of the non-uniform in situ stress acting on the casing is obtained as follows:

$$p_o = -s_1 + \frac{2|m^2 s_3 - 1 + m^2 s_2|}{1 - m^2} \quad (9)$$

The annulus fluid inside the casing in the overlaying and stratum sections is the drilling fluid used before the next spud cementing operation. Considering the effect of hydrostatic pressure and annulus pressure, the calculation

formula of the casing internal pressure in the overlaying and stratum sections is as follows:

$$p_i = 0.00981\rho_{nmax}h + p_{ia} \tag{10}$$

where ρ_{nmax} denotes the maximum drilling fluid density in the next spuds, g·cm^{-3}; p_{ia} denotes the annulus pressure inside of the casing, MPa; h denotes the vertical depth, m.

The research (Gao 2007) shows that the casing is affected by the payload, and the Mises equivalent stress of the casing is the minimum when the internal pressure acting on the casing is equal to the external extrusion pressure. The load reduction ratio of the cement sheath remains unchanged when the elastic modulus, Poisson's ratio, thickness, and other parameters of the cement sheath are determined. Due to the regional difference of in situ stress, it is necessary to calculate the casing payload and judge the reliability according to the actual situation.

2.2 Calculation Model of Casing Strength

The K-T formula considers the influence of manufacturing tolerance, material strain hardening index, and manufacturing defects on the strength (Galambos and Ravindra 1978), and the calculated result is close to the actual strength. The calculation formula of effective anti-extrusion strength of casing under the condition of triaxial stress is as follows (The detailed calculation process of Formula (11) is shown in Appendix C):

$$q_{ca} = \frac{(\Delta p_e + \Delta p_y) - \sqrt{(\Delta p_e - \Delta p_y)^2 + 4\Delta p_e \Delta p_y H_t}}{2(1 - H_t)} \tag{11}$$

where q_{ca} denotes the effective anti-extrusion strength, MPa; H_t denotes the manufacturing residual stress influence factor.

The effective anti-internal-pressure strength of casing under triaxial stress is calculated as follows (The detailed calculation process of Formula (12) is shown in Appendix D):

$$q_{ba} = \boldsymbol{min}\left(\frac{1}{2}(p_M + p_{refT}), p_M\right) \tag{12}$$

where q_{ba} denotes the effective anti-internal-pressure strength, MPa.

2.3 Quantitative Evaluation Method of Casing Reliability of HTHP Wells

2.3.1 Uncertainty Analysis of Load and Strength

There is uncertainty in the calculation results of traditional casing load and strength models due to the uncertainty of downhole information and the randomness of manufacturing tolerance values of the casing performance parameters. Based on the Monte Carlo simulation method and probability statistics theory, firstly, probability statistics are performed on the indirect or direct measurement parameters affecting casing strength and load. Next, a random sampling simulation is performed. Finally, we can obtain the probability distribution intervals of casing load and strength. The basic process is shown in Fig. 3 and described as follows.

1. Determining the probability distribution functions of parameters, which affect the uncertainty of casing load and strength. The parameters that affect casing load mainly include rock mechanics parameters, in situ stress, drilling fluid density, and annulus pressure. The influencing parameters of casing strength mainly include casing performance parameters, wellbore temperature, and casing load. According to the stratigraphic information, the stratified horizontal statistics are carried out on geo-pressure, rock mechanical parameters, in situ stress, and wellbore temperature. Thus, we can obtain the probability distribution functions $f_{i,j}(x)$ at different layers, where f represents the probability density function (according to (Li et al. 2021), the distribution is set as normal in this paper), i represents the parameter type, and j represents the stratum layer. Based on the probability distributions of geo-pressure and wellbore pressure, using the Monte-Carlo simulation method (Harrison 2010), we can obtain the probability distribution of annulus pressure $f_i(x)$. For the casing performance parameters, the random distribution characteristics of each performance parameter of the casing are given according to the experimental results of different sizes of casing in the ISO standard (10,400, 2007; Galambos and Ravindra 1978), as shown in Table 1. Thus, we can obtain the probability density function $f_i(x)$ of each performance parameter.

2. To perform the load uncertainty analysis of different working conditions or different casing sections, the probability density functions $f_{i,j}(x)$ or $f_i(x)$ of the corresponding influencing parameters are matched by combining with the wellbore structure and the WLC casing load calculation model. Using the Monte-Carlo simulation method, taking the probability density functions of matched influencing parameters into the load calculation model, we can obtain the casing load probability density functions $f_{i,j}(y), i \in \{p_o, p_i\}$ of the corresponding working conditions or casing sections. Finally, the type of casing payload is determined according to the mean value of external extrusion pressure and internal pressure, and the probability density functions $f_{i,j}(y), i \in \{p_{ce}|p_{be}\}$ of the casing payload are obtained through the formula (13).

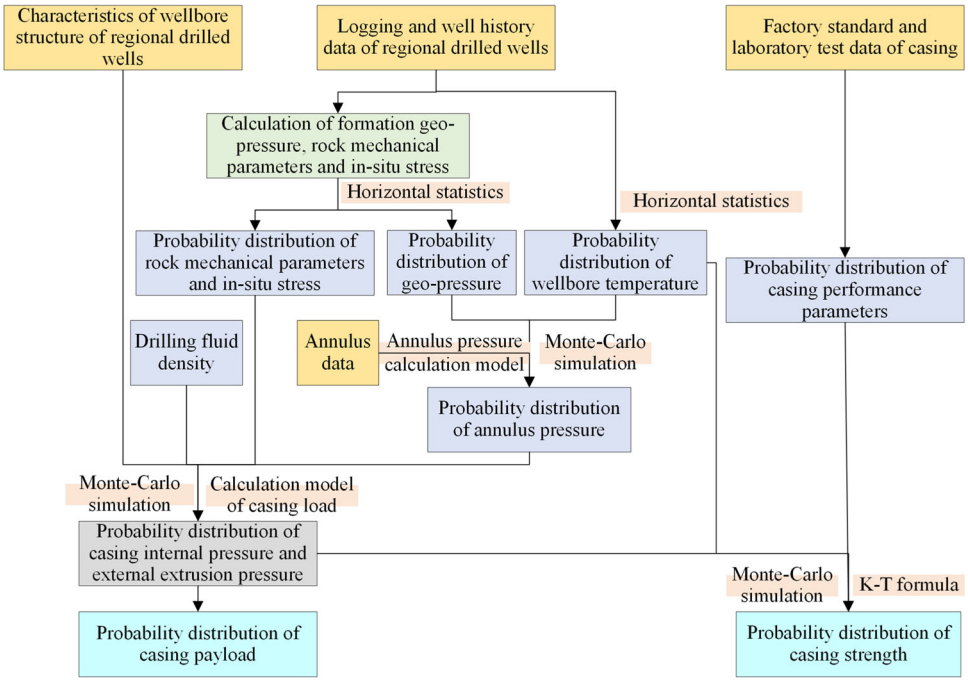

Fig. 3 Flowchart of uncertainty analysis of casing load and strength

Table 1 Random distribution characteristics of casing pipe performance parameters

Performance parameters	Mean value/nominal value	Variation coefficient
Outer diameter D_c	1.0025	0.0019
Wall thickness δ	1.0000	0.0310
Yield strength Y_p	1.09	0.022
Elastic modulus E_c	1.00	0.035
Poisson's ratio v_c	1.00	0.025

$$\begin{cases} \mu_{p_{ce},j} = \mu_{p_o,j} - \mu_{p_i,j} \\ \sigma_{p_{ce},j} = \sqrt{\sigma^2_{p_o,j} + \sigma^2_{p_i,j}} \end{cases}$$

or

$$\begin{cases} \mu_{p_{be},j} = \mu_{p_i,j} - \mu_{p_o,j} \\ \sigma_{p_{be},j} = \sqrt{\sigma^2_{p_i,j} + \sigma^2_{p_o,j}} \end{cases}$$

(13).

where $\mu_{p_o,j}$, $\mu_{p_i,j}$, $\mu_{p_{ce},j}$, $\mu_{p_{be},j}$ denote the mean values of casing external extrusion pressure, internal pressure, effective external extrusion pressure, and effective internal pressure, respectively, MPa; $\sigma_{p_o,j}$, $\sigma_{p_i,j}$, $\sigma_{p_{ce},j}$, $\sigma_{p_{be},j}$ denote the standard deviation of casing external extrusion pressure, internal pressure, effective external extrusion pressure, and effective internal pressure, respectively, MPa;

3. Similarly, for the casing strength, the probability density functions of casing load and casing pipe performance parameters are taken into the strength calculation model. Using the Monte-Carlo simulation method, we can obtain the probability density functions: $f_{q_{ca},j}(y)$ (effective anti-extrusion strength) and $f_{q_{ba},j}(y)$ (effective anti-internal-pressure strength).

2.3.2 Quantitative Evaluation Method

The safety factor method is the traditional method for evaluating the reliability of the casing, which takes the ratio of the casing strength to the load as the safety factor and compares it with the specified threshold to judge whether the casing is safe. Due to the uncertainty of casing load and strength, even if the safety factor is greater than 1, there is still a certain degree of unreliability. According to the stress–strength interference theory (Liao et al. 2012), the reliability R is defined as the probability P that the casing strength is greater than the casing load, namely,

$$R = P(q > p) = P(q - p > 0) \tag{14}$$

The stress–strength interference theory believes that reliability is the ability of casing to resist failure under

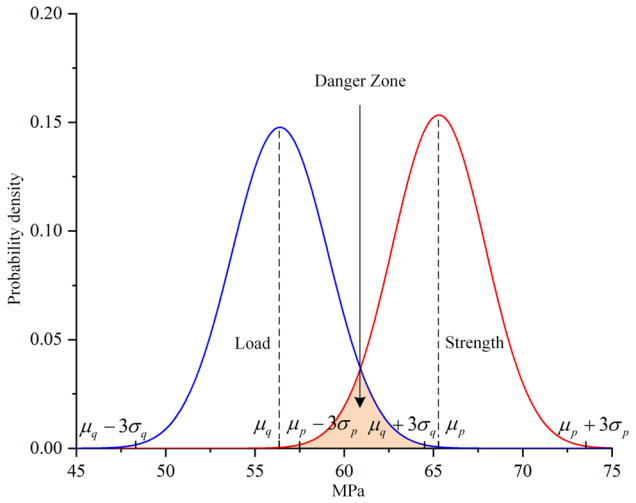

Fig. 4 Interference model of casing load and strength probability distribution

given operating conditions, which is the result of the interaction between stress and strength. Due to the randomness of the factors affecting stress and strength, stress and strength exhibit dispersion characteristics. The probability distribution of stress and strength is obtained through Monte Carlo simulation. Compared to traditional methods such as finite element analysis and safety factors, the stress–strength interference theory considers the impact of uncertainty and quantitatively evaluates the reliability of the casing. As shown in Fig. 4, the casing load p and strength q are normally distributed, and the overlapping shaded part represents the casing failure risk probability F. Since the reliability of the casing and the risk probability are reciprocal events, then,

$$F = 1 - R \tag{15}$$

The mean values and standard deviations of casing load p and strength q can be obtained from Sect. 2.3.1. The interference variable is defined as $z = q - p$, and it can be inferred that the interference variable z also obeys the normal distribution. Therefore, the calculation formula for casing reliability is:

$$\begin{aligned} R &= \int_{-\infty}^{\infty} f_p(p)\left[\int_{p}^{\infty} f_q(q)dq\right]dp \\ &= \int_{0}^{\infty} \frac{1}{\sqrt{2\pi}\sigma_z}\exp\left[-\frac{(z-\mu_z)^2}{2\sigma_z^2}\right]dz \end{aligned} \tag{16}$$

where $\mu_z = \mu_q - \mu_p$, $\sigma_z = \sqrt{\sigma_q^2 + \sigma_p^2}$.

3 Case Study

3.1 Formation Background

Well A is located in the Yingqiong Basin, South China Sea, with a true vertical depth (TVD) of 4110m. The well bottomhole temperature is 167.9 °C, and the bottomhole pressure is 86 MPa. The well structure and casing related data are shown in Table 2.

3.2 Influence of HTHP Environment on Casing Load and Strength

In HTHP wells, temperature and other factors will affect the yield strength, elastic modulus, and other parameters of the casing, thus affecting the casing strength. To explore the effect of temperature on the casing strength, the high-temperature tensile test is carried out. By stretching the test pieces at different temperatures, the stress–strain curves and the yield indexes of plastic strain at different temperatures can be obtained. Thus, we can obtain the change rules of the elastic modulus and yield strength of the casing with temperature. As shown in Fig. 5a, taking N80-grade steel casing as an example, the effect of temperature on the yield strength and elastic modulus of the casing is almost linear. And the influence degree is related to the steel materials. For different steel grade casings, the relational expressions of elastic modulus and yield strength with temperature are established, respectively.

The correction formula of elastic modulus affected by temperature is as follows:

$$E_c' = E_c(1 - K_e)T \quad (T > 25) \tag{17}$$

where T denotes the temperature, °C.

The correction formula of yield strength affected by temperature is as follows:

$$Y_p' = Y_p(1 - K_y)T \quad (T > 25) \tag{18}$$

Taking 13–3/8-inch N80-grade casing, the change rule of casing strength affected by temperature is obtained by comprehensively considering the influence of temperature on yield strength and elastic modulus, as shown in Fig. 5b. It can be seen that the anti-extrusion strength is less affected by temperature, and the strength value decreases slightly even when the temperature exceeds 300 °C. While the anti-internal-pressure strength is more obviously affected by temperature. In the HTHP environment, the failure risk of anti-internal-pressure of the casing will increase due to the influence of temperature when the casing is subject to effective internal pressure.

The influence of the HTHP environment on casing load is not only by changing the annulus pressure and drilling fluid rheological parameters but also by affecting the

Table 2 Well structure and casing data of well A

Spud	Conductor	1st spud	2nd spud	3rd spud	4th spud
Casing size/in	30	20	13–3/8	9–5/8	Open-hole
Casing depth/m	197	1300	3180	3940	4100
Depth of cement surface/m	Mudline	Mudline	1100	2980	/
Bottomhole temperature/°C	20	78	150	182	188
Unit weight/ppf	309.7	106.5/ 133	68	53.5	/
Steel grade	Q235B	K55	N80	Q125	/
Wall thickness/mm	25.4	12.7/ 16.1	12.2	13.8	/
Geo-pressure coefficient/g·cm^{-3}	1.00	1.00	1.00–1.68	1.68–1.82	1.82–2.00
Drilling fluid density/g·cm^{-3}	1.03–1.08	1.03–1.08	1.03–1.75	1.68–1.85	1.85–2.06
Elastic modulus/GPa	206	210	198	207	/
Yield strength/MPa	235	379.4	552.4	862.3	/
Poisson's ratio	0.25	0.3	0.26	0.28	/

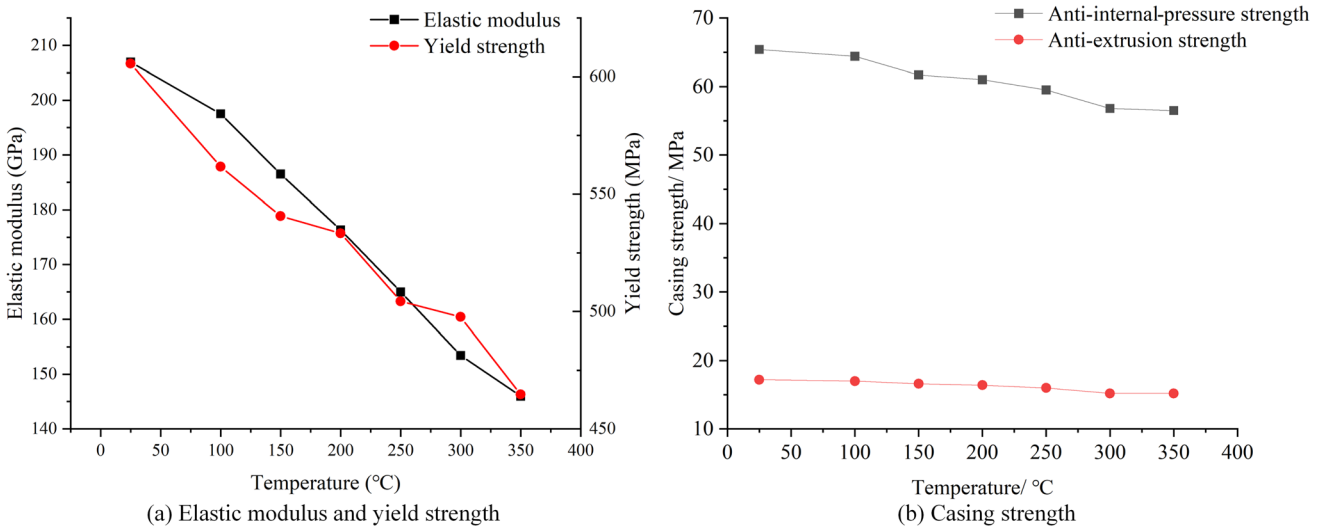

Fig. 5 Diagram of casing strength and performance parameters changing with temperature

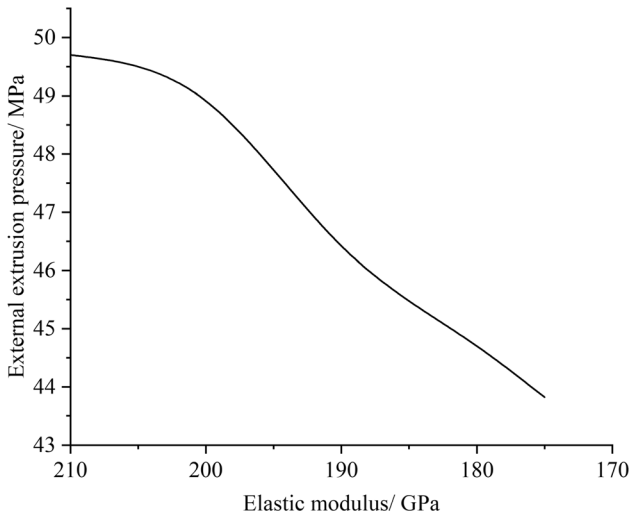

Fig. 6 Diagram of casing external extrusion pressure changing with elastic modulus

casing performance parameters. In the production stage, the elastic modulus of casing will decrease with the rise of downhole temperature. And based on the aforementioned calculation model of casing equivalent external extrusion pressure, the external extrusion pressure also decreases under the condition of constant in situ stress, as shown in Fig. 6. It can be found that when the temperature reaches 200 °C, the elastic modulus of the casing decreases to 175 GPa, then the external extrusion pressure will decrease by 5.7 MPa. If the casing is subject to effective internal pressure, its payload will increase, which reduces its reliability of anti-internal-pressure.

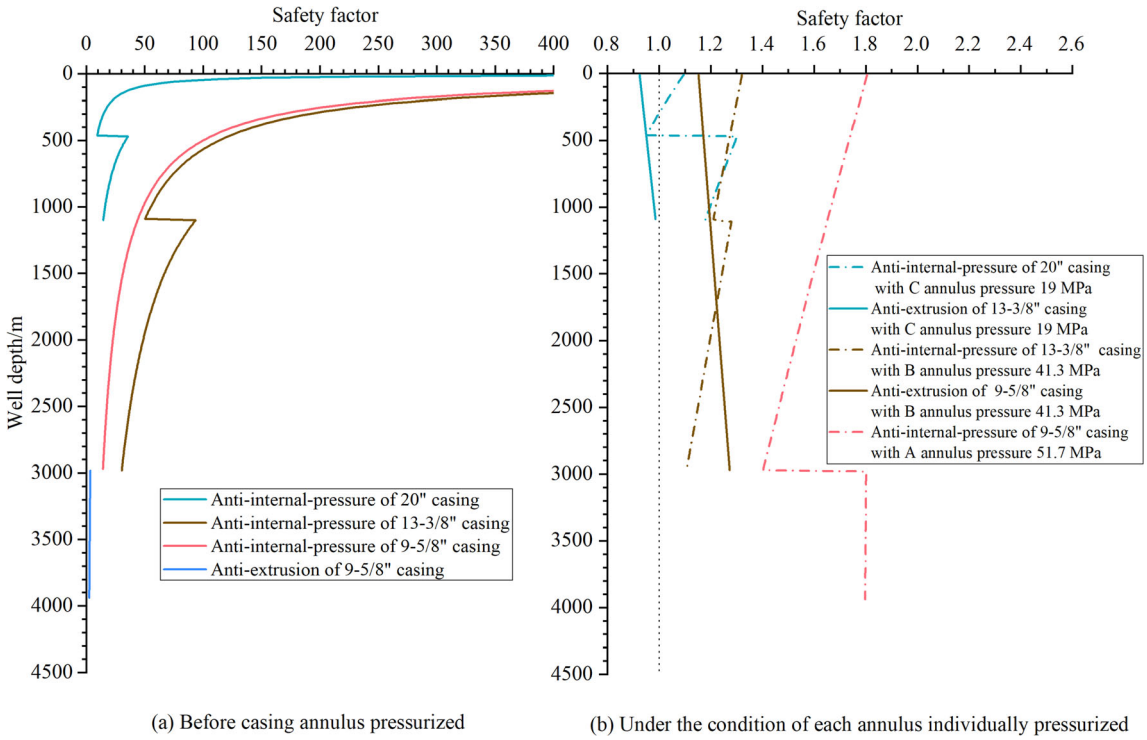

(a) Before casing annulus pressurized (b) Under the condition of each annulus individually pressurized

Fig. 7 Distribution diagram of casing safety factor at the production stage of well A

3.3 Reliability Evaluation in the Production Stage

3.3.1 Casing Safety Factor Before Annulus Pressurized

For the production stage, the casing safety factor before and after the annulus pressurization is analyzed by calculating the casing load and strength. Figure 7a shows the distribution of safety factor before the annulus pressurization. It can be found from Table 2 and Fig. 7a that the 20-inch casing only includes the stratum section, due to the small in situ stress in the shallow formation and the load reduction effect of the cement sheath, it is subject to the effective internal pressure. The lowest point of the safety factor of anti-internal-pressure is at 460m (that is, the boundary between the casings with two kinds of wall thickness). Due to the relatively high density of the inside drilling fluid, the 13–3/8-inch casing is generally affected by the effective internal pressure, which decreases with the increasing well depth. The safety factor of anti-internal-pressure suddenly increases at 1100m (that is, the cement surface outside the casing) due to the impact of in situ stress, and the minimum safety factor of anti-internal-pressure appears at 2980m (that is, the cement surface inside the casing). Similarly, the unsealed section at the upper part of 9–5/8-inch casing is subject to effective internal pressure. While the overlaying and stratum sections at the lower part of 2980m, due to the large in situ stress of deep formation, are subject to effective external extrusion pressure, even under the action of cement sheath load reduction.

3.3.2 Reliability Analysis After Annulus Pressurization

The output is set to 20×10^4 m^3/d, and the production period is set to 90 days (annulus pressure tends to be stable). The trapped annulus pressure and sustained annulus pressure of annuli A, B, and C are calculated, respectively. Selecting the greater values among the two kinds of annulus pressure in each annulus, the casing load and strength after each annulus is individually pressurized are calculated to perform the reliability analysis. The results are shown in Fig. 7b and Table 3. It can be found that the overall trend and weak points of the casing safety factor of anti-internal-pressure remain the same after each annulus is individually pressurized. In addition, the annulus pressure will also affect the anti-extrusion reliability of the casing inside the annulus. It can be seen that the minimum anti-extrusion safety factors of the 13–3/8-inch casing and the 9–5/8-inch casing are at the wellhead. Since the density of the liquid in the inner annulus of the casing is greater than that of the outer annulus, the effective external extrusion pressure gradually decreases with the increasing well depth. The casings on both sides of annuli A and B can achieve safe production after the annulus is pressurized. While the pressure in annulus C reaches 19 MPa, which

Table 3 Reliability analysis results of well A under each annulus individually pressurized

Casing size/ in	Weak point/ m	Risk type	Annulus pressure/ MPa	Effective load/ MPa	Strength/ MPa	Safety factor	Reliability
20	460	Anti-internal-pressure	C/ 19	23.32	22.18	0.951	0.67
13–3/8	0	Anti-extrusion	C/ 19	19	17.56	0.924	0.55
13–3/8	2980	Anti-internal-pressure	B/ 41.3	52.1	57.57	1.105	0.97
9–5/8	0	Anti-extrusion	B/ 41.3	41.3	47.578	1.152	0.99
9–5/8	2980	Anti-internal-pressure	A/ 51.7	54.03	75.75	1.402	0.99

poses a safety challenge to the anti-extrusion at the wellhead of 13–3/8-inch casing inside the annulus and the anti-internal-pressure at 460m of 20-inch casing outside the annulus. In fact, after the well is put into production for a period, the casing on both sides of the C annulus is slightly deformed, which shows the effectiveness of the proposed evaluation method.

It can be seen from Table 3 that under the allowable safety factor, the casing weak points still have certain unreliability. According to the characteristics of the normal distribution cumulative probability density function, when the reliability $R = 1$, the interference variable z is a positive infinite value. Therefore, assuming that $R = 0.99$, the casing is safe and reliable. To make the reliability of overall casings reach 0.99, through multiple back-calculations, the MAAPs of annuli A, B and C are 76MPa, 40.5MPa, and 13.8Mpa.

3.4 Failure Risk Analysis in the Well Construction Stage

To ensure the WLC reliability of the casing in HTHP wells, the failure risks of casing in each extreme condition are analyzed for the well construction stage. And the MAHDs of casing safety under the conditions of lost circulation, gas intrusion, and casing running are recommended. The results are shown in Figs. 8, 9, 10.

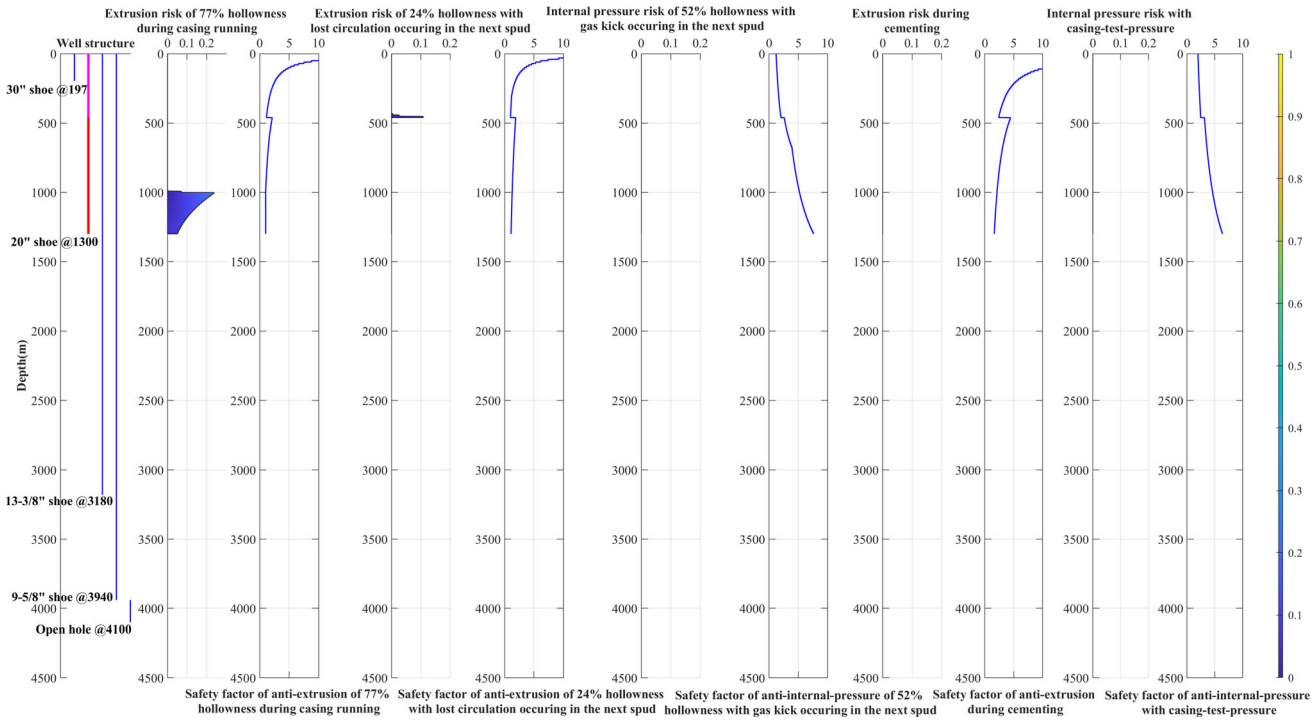

Fig. 8 Reliability distribution diagram of 20-inch casing during the well construction stage

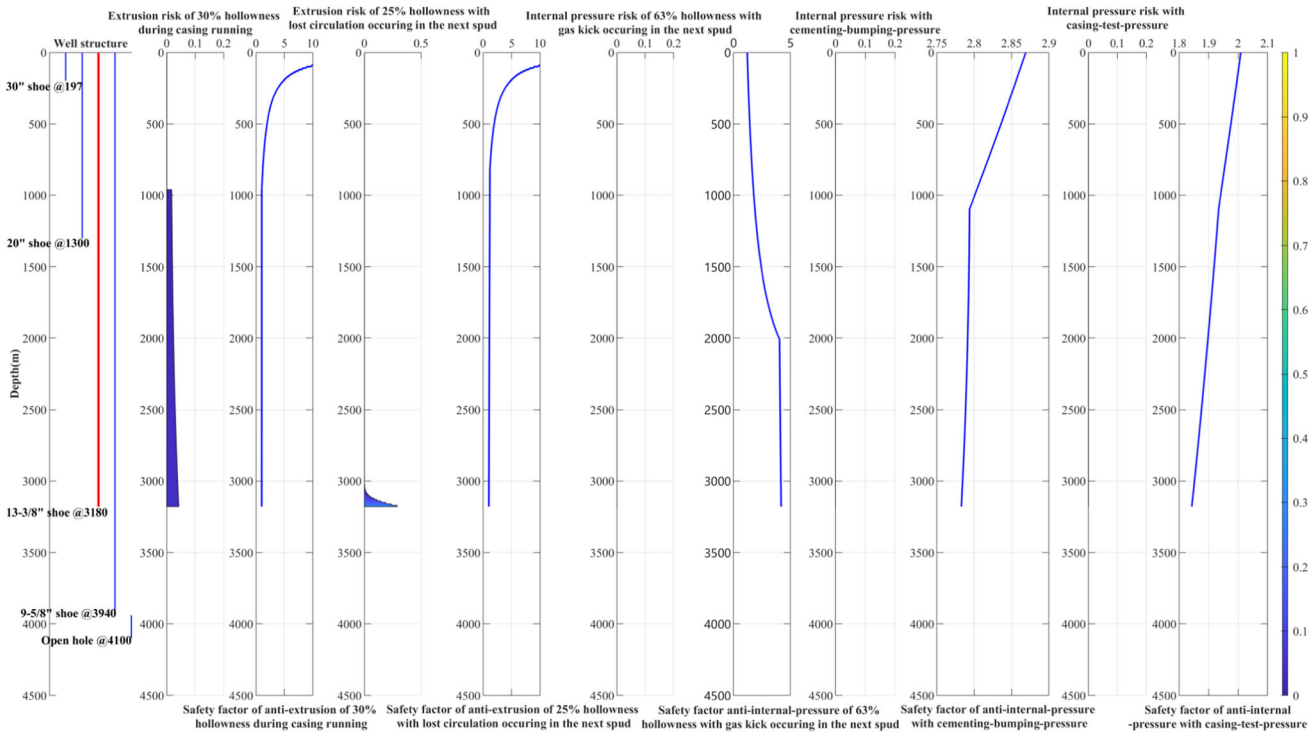

Fig. 9 Reliability distribution diagram of 13–3/8-inch casing during the well construction stage

It can be seen from Fig. 8 that, for the 20-in casing, the MAHD during the casing running process is 77%, and the dangerous section is the hollowing surface, where the anti-extrusion safety factor is 1 and the reliability is about 0.8. When lost circulation occurs in the next spud, the MAHD is 24%, and the dangerous section is at the hollowing surface, with an anti-extrusion safety factor of 1 and a reliability of 0.89. During the gas kick process in the next spud, the MAHD is 52%, and the dangerous section is at the wellhead, with an anti-internal-pressure safety factor of 1.2 and a reliability of 0.99. The internal-string cementing technique is adopted for the 1st spud, so there is no displacement pressure, the casing is subject to effective external extrusion pressure, and the minimum anti-extrusion safety factor appears at the bottom of the well. During the casing-pressure-testing process, the casing is mainly affected by effective internal pressure, and the minimum safety factor of anti-internal-pressure appears at the wellhead.

As for the 13–3/8-in casing, it can be seen from Fig. 9 that the MAHD during the casing running process is 30%, and the dangerous section is at the casing shoe, with an anti-extrusion safety factor of 1 and a reliability of 0.9. In the process of lost circulation in the next spud, the MAHD is 25%, and the dangerous section is at the bottom of the well, with an anti-extrusion safety factor of 1 and anti-extrusion reliability of 0.7. In the process of gas kick in the next spud, the MAHD is 63%, and the dangerous section is at the wellhead, with an anti-internal-pressure safety factor of 1.2 and anti-internal-pressure reliability of 0.99. The double-rubber-plug cementing technique is adopted in the 2nd spud, with a bumping-pressure of 20 MPa, the casing is subject to effective internal pressure. The safety factor does not fluctuate much in the whole casing, and the minimum anti-internal-pressure safety factor appears at the casing shoe. In the process of the casing-pressure-testing, the curve of the safety factor of anti-internal-pressure has little difference with that of cementing, and the minimum anti-internal-pressure safety factor also appears at the casing shoe.

For the 9–5/8-in casing, it can be seen from Fig. 10 that the MAHD is 67% during casing running, and the dangerous section appears at the bottom of the well, with an anti-extrusion safety factor of 1 and anti-extrusion reliability of 0.8. The MAHD is 66% when lost circulation occurs in the 4th spud drilling process, and the dangerous section appears at the casing shoe, with an anti-extrusion safety factor of 1 and reliability of 0.5. When gas kick occurs during the drilling process of the 4th spud, the MAHD is 99%, the minimum anti-internal-pressure safety factor at the wellhead is 1.2, and the reliability is 0.99. In the process of cementing and casing-pressure-testing, the casing meets the requirements of reliability, the safety factor of the whole casing section is similar, and the weak point is at the casing shoe.

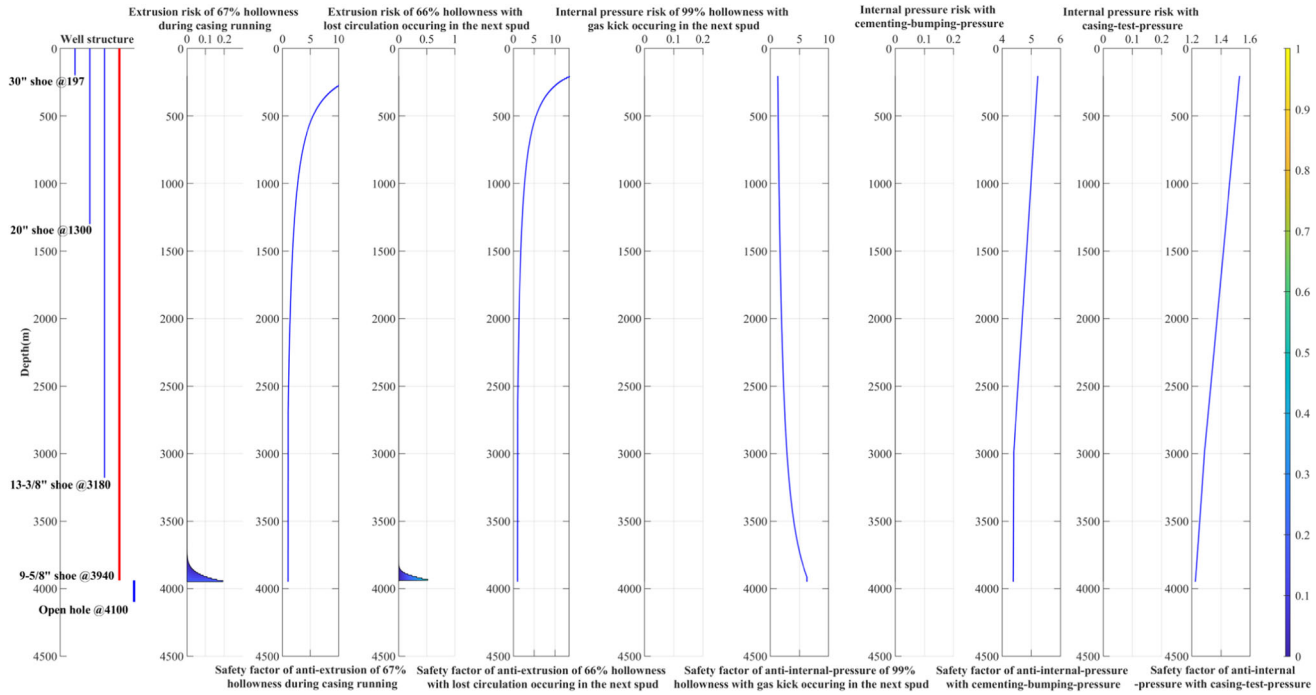

Fig. 10 Reliability distribution diagram of 9–5/8-inch casing during the well construction stage

It can be found from the above analysis results that, within the allowable range of the safety factor, there are still some risks at the casing shoe under the condition of lost circulation and casing running. To ensure the reliability of the casing to reach 0.99, the recommended MAHDs for each spud are given through back-calculation under the conditions of casing running, lost circulation, and gas kick. For the 20-inch casing, the MAHDs are 74, 21, and 52%, respectively. For the 13–3/8-inch casing, the MAHDs are 30, 20, and 63%, respectively. And for the 9–5/8-inch casing, the MAHDs are 64, 64, and 99%, respectively.

It is concluded that the casing failure risk of the whole well mainly occurs in the conditions of casing running and lost circulation. The MAHDs of 20-inch and 13–3/8-inch casings are low, which fails to meet the requirement of more than 30% hollowing. In addition, in the long-term production stage, the MAAP of annulus C is low, and there will be certain risks when annulus C is pressurized. It is recommended to increase the length of the thicker wall section of the 20-inch casing, increase the wall thickness of the 13–3/8-inch casing, increase the steel grade of the 13–3/8-inch casing or reduce the running depth of the 13–3/8-inch casing.

4 Conclusion

The evaluation method proposed in this paper investigates the effects of annulus pressure, non-uniform in situ stress, drilling extreme conditions, and the HTHP environment, which can be used to calculate the MAAP and MAHD under existing production and drilling plans, thus helping to optimize production and casing strength design. Compared to the conventional casing reliability evaluation methods, the proposed method considers the WLC casing load variation of HTHP wells, the impact of the HTHP environment, and the information uncertainty of casing load and strength. The detailed conclusions are as follows:

1. In the HTHP environment, high temperature will reduce the elastic modulus and yield strength of the casing, thereby reducing the casing strength of anti-extrusion and anti-internal-pressure. If the casing is subject to effective internal pressure, the reliability of anti-internal-pressure will decrease. Design suggestion: when the formation temperature exceeds 100 °C, the casing strength should be designed with a margin to avoid high temperature reducing reliability.
2. For the well construction stage, the weak points of casing anti-extrusion are located at the casing shoe during casing running, lost circulation, cementing, and casing-pressure-testing conditions, and the weak point of casing anti-internal-pressure is located at the wellhead in case of gas kick. Under the hollowing

degree with allowable safety factors, there is still some risk in the casing running and lost circulation conditions. The MAHDs were calculated to ensure casing safety under the existing drilling plan. Design suggestion: the casing strength at weak points should be strengthened accordingly if in leak-prone geological conditions such as narrow safety pressure windows and fractured strata.

3. For the production stage, before and after annulus pressurization, the overall trend of the casing safety factor of anti-internal-pressure remains the same and decreases with increasing well depth. The weak points exist at the inner cement surface or boundary point of different wall thickness casings. The risk of casing extrusion after annulus pressurization increases with decreasing well depth, the weak points are located at the wellhead. Under the existing production plan, the MAAPs were calculated for production optimization. Annulus pressure is common in the production stage of HTHP wells, if it can be considered in the casing-strength design, the casing reliability will be improved.

Appendix A: Trapped Annulus Pressure Calculation Model

For a trapped annulus at a certain well depth, the pressure change of this annulus section depends on the average changes of temperature and volume of this annulus section. The pressure–volume coupling under the condition of the multi-layer annulus is considered for calculation. The trapped annulus pressure change is calculated as follows:

$$\Delta p = \frac{\alpha}{\kappa_{\mathrm{T}}}\Delta T - \frac{\Delta V_{\mathrm{ann}}}{\kappa_{\mathrm{T}} V_{\mathrm{ann}}} + \frac{\Delta V_l}{\kappa_{\mathrm{T}} V_l} \tag{A1}$$

where ΔP denotes the trapped annulus pressure, MPa; α denotes the isobaric expansion coefficient of fluid, $^{\circ}\mathrm{C}^{-1}$; κ_{T} denotes isothermal compression coefficient of fluid, MPa^{-1}; V_{ann} denotes the annulus volume, m^3; V_l denotes the annulus fluid volume, m^3; ΔT denotes the annulus average temperature change, °C.

Appendix B: Sustained Annulus Pressure Calculation Model

$$\begin{cases} 10^{-4} R_s A H_l + V_{gan} = V_g \\ \dfrac{V_{gan} T_{an} Z_{an} p_a}{p_{an} Z_a T_a} + 10^{-4} A H_l (1 - p_{an} K_T) = V_{an} \end{cases} \tag{B1}$$

$$V_g = 10^{-6} \sum_{j=1}^{J} Q_j t_a \tag{B2}$$

where p_{an} denotes the sustained annulus pressure, MPa; R_s denotes the gas solubility in annulus liquid, $\mathrm{m}^3 \cdot \mathrm{m}^{-3}$; A denotes the cross-sectional area of cement sheath, m^2; H_l denotes the initial height of the liquid column, m; V_{gan} denotes the standard volume of the air column in the upper annulus, m^3; V_g denotes the total volume of gas entering the annulus under standard conditions, m^3; T_{an} denotes the annulus upper temperature, K; Z_{an} denotes the compressibility factor of annulus gas, dimensionless; p_a denotes the gas pressure under standard conditions, MPa; Z_a denotes the gas compression factor under standard conditions, dimensionless; T_a denotes the gas temperature under standard conditions, K; K_T denotes the isothermal compression coefficient of annulus liquid, MPa^{-1}; V_{an} denotes the total annulus volume, m^3; Q_j denotes the gas flow in the jth period, $\mathrm{m}^3 \bullet \mathrm{s}^{-1}$; J denotes the total time-phased, dimensionless; t_a denotes the length of period, s.

Supposing that the gas migration in the cement sheath is one-dimensional unstable seepage of a single medium, the seepage formula is as follows:

$$\frac{\partial}{\partial x}\left(\frac{p}{\mu Z}\frac{\partial p}{\partial x}\right) = \frac{\varphi C(p)\mu}{K_e}\frac{p}{\mu Z}\frac{\partial p}{\partial t} \tag{B3}$$

where x denotes the coordinate system established along seepage direction, cm; p denotes the pressure, 10^5 Pa; μ denotes the gas viscosity, mPa•s; Z denotes the gas compression factor, dimensionless; φ denotes the porosity, dimensionless; $C(p)$ denotes the isothermal compression coefficient of gas, $_{(105\ \mathrm{Pa})\text{-}1;}$ K_e denotes the comprehensive permeability of cement sheath, $\mu\mathrm{m}^2$; t denotes the time, s.

If the period is short enough, the annulus pressure can be regarded as a fixed value, and the gas seepage velocity can be obtained as follows:

$$Q_j = 10^{-5}\frac{K_e A}{2L}\frac{T_r Z_a}{T_{an}\overline{Z}\,\overline{\mu} p_a}\left[p_p^2 - (p_l + p_{anj-1})^2\right] \tag{B4}$$

where L denotes the length of cement sheath, cm; $\overline{Z}$ denotes the gas compressibility factor under average seepage pressure difference, dimensionless; $\overline{\mu}$ denotes the gas viscosity under average seepage pressure difference, mPa•s; p_p denotes the gas reservoir pressure, MPa; p_l denotes the annulus liquid column pressure, MPa; p_{anj-1} denotes the annulus pressure in the j-1th period, MPa; T_r denotes the gas reservoir temperature, K.

Appendix C: The Explanation of the Calculation Process of Formula (11)

The calculation formulas of the intermediate parameters of Formula (11) are:

$$\Delta p_e = k_e 2E_c/[(1-v_c^2)(D_c/\delta)(D_c/\delta-1)^2] \tag{C1}$$

$$\Delta p_y = \begin{cases} (\Delta p_{yvem} + \Delta p_{yT})/2 & \Delta p_{yvem} > \Delta p_{yT} \\ \Delta p_{yvem} & \Delta p_{yvem} \le \Delta p_{yT} \end{cases} \tag{C2}$$

In formula (C2),

$$\Delta p_{yT} = k_y 2Y_p \delta/(D_c - \delta) \tag{C3}$$

wherek_e, k_y denote the design elastic collapse and design yield collapse parameters, respectively, dimensionless; D_c, δ denotes outer diameter and wall thickness of casing, respectively, mm; Y_p denotes casing yield strength, MPa.

In addition, Δp_{yvem} needs to be iteratively calculated with p_o as the iterative variable until the following equations are satisfied:

$$\begin{cases} \Delta p_{yvem} = \sqrt{4/3} k_y Y_p [\delta/(D_c-\delta)]\left\{1-\left[F_{eff}/(\pi\delta(D_c-\delta)\sigma_a)\right]^2\right\}^{1/2} \\ \Delta p_{yvem} = p_o - p_i \\ F_{eff} = \pi\delta(D_c-\delta)\sigma_a - p_i A_i + p_o A_o \end{cases} \tag{C4}$$

where σ_a denotes the axial casing stress, MPa; A_o, A_i denote the external and internal sectional area of casing, respectively, m^2.

Appendix D: The Explanation of the Calculation Process of Formula (12)

The calculation formulas of the intermediate parameters of Formula (12) are:

$$p_{refT} = 2^{1-n} Y_p \frac{\delta}{(D_c-\delta)} \tag{D1}$$

$$p_M = p_{refM}\left\{1-\left((4^{1-n}-1)/3^{1-n}\right)\left[F_{eff}/\left(\pi\delta(D_c-\delta)Y_p\right)\right]^2\right\}^{1/2} \tag{D2}$$

where n denotes the material hardening coefficient, dimensionless.

In addition, p_M needs to be calculated iteratively with F_{eff} as the iteration variable until p_M converges to a certain precision. The calculation equations are as follows:

$$\begin{cases} p_{refM} = \dfrac{4}{3^{\frac{1+n}{2}}} Y_p \dfrac{\delta}{(D_c-\delta)} \\ F_{eff} = \pi\delta(D_c-\delta)\sigma_a + p_o\pi\delta(D_c-\delta) - p_M\delta \\ (D_c-\delta)/[\delta(D_c-\delta)]\dfrac{\pi}{4}[D_c-2\delta]^2 \end{cases} \tag{D3}$$

Acknowledgements This research is sponsored by Beijing Nova Program (20230484365).

Funding This work was supported by a Grant (Grant No. 20230484365) from Beijing Nova Program.

Declarations

Conflict of interest The authors declare that they have no known competing financial interests or personal relationships that could have appeared to influence the work reported in this paper.

References

10400, I.T. (2007) Petroleum and Natural Gas Industries—Equations and calculations for the properties of casing, tubing, drill pipe and line pipe used as casing or tubing. ISO Geneva, Switzerland

Bailing Z, Jin Y, Xiaolong H, Zhiqiang H, Li H (2015) Adaptability evaluation of calculation model of annular pressure of deepwater wellhole. Oil Drill Prod Technol 37(1):56–59

Bo Z, Zhichuan G, Qi Z (2015) Prediction and analysis on annular pressure of deepwater well in the production stage. Acta Petrolei Sinica 36(8):1012

Cao L, Sun J, Zhang B, Lu N, Xu Y (2022) Sensitivity analysis of the changing law of temperature profile in the production string of the high-pressure high temperature gas well considering the coupling relation among the gas flow friction, gas properties, temperature and pressure. Front Phys 10:1050229

Dong G, Chen P (2017) A review of the evaluation methods and control technologies for trapped annular pressure in deepwater oil and gas wells. J Natural Gas Sci Eng 37:85–105

Galambos TV, Ravindra MK (1978) Properties of Steel for Use in LRFD. J Struct Div 104(9):1459–1468

Gao J (2007) Study on Reliability and Risk Assessment of Casing in Complex Well Status, China University of Petroleum

Gu Q et al (2021) A novel dilution control strategy for gas kick handling and riser gas unloading mitigation in deepwater drilling. J Petrol Sci Eng 196:107973

Guan Z et al (2018) A new quantitative evaluation method for drilling risk based on uncertainty analysis. Kuwait J Sci 45(3)

Guohua W, Jiyou X, Keli Y (2012) Study on the effect of non-uniformity load and casing eccentricity on the casing strength. Energy Proc 14:285–291

Harrison RL (2010) Introduction to monte carlo simulation. In: AIP conference proceedings. American Institute of Physics, pp 17–21

Jaimes JP, Croy S, Bouguetta M, Williford M (2022) Drilling fluids design and field deployment for the first HTHP Deepwater production project in the US Gulf of Mexico. IADC/SPE international drilling conference and exhibition. OnePetro

Jin Y et al (2013) Prediction model of casing annulus pressure for deepwater well drilling and completion operation. Pet Explor Dev 40(5):661–664

Kuanhai D et al (2022) Study on residual strength and life prediction of corroded tubing based on thermal-mechanical coupling XFEM. Ocean Eng 255:111450

Li M et al (2021) Safety and reliability evaluation of casing in ultra-deep well based on uncertainty analysis of extrusion load. Process Saf Environ Prot 148:1146–1163

Lian Z, Luo Z, Yu H, Liu Y, He Y (2018) Assessing the strength of casing pipes that contain corrosion pit defects. Southwest Petrol Univ Sci Technol Edn 40(2):159

Liao H, Guan Z, Long G (2012) Quantitative risk assessment on safety and reliability of casing strength for oil and gas wells. Energy Proc 17:429–435

Liu H et al (2019) Research and practice of full life cycle well integrity in HTHP well, Tarim Oilfield. In: International petroleum technology conference. OnePetro.

Ming L, Jiang W, Haodong C, Ping X (2019) Ultra-high temperature high pressure drilling technology for narrow safety density

window strata in the western South China. Petrol Drilling Techniq 47(1):8–12
Muoghalu A, Ansa J, Dosunmu A (2020) Probability approach to casing design using monte carlo simulation. In: SPE Nigeria annual international conference and exhibition. OnePetro.
Oudeman P, Kerem M (2006) Transient behavior of annular pressure build-up in HP/HT wells. SPE Drill Complet 21(04):234–241
Qian F, Gao D (2011) A mechanical model for predicting casing creep load in high temperature wells. J Nat Gas Sci Eng 3(3):530–535
Seymour K, MacAndrew R (1993) The design, drilling, and testing of a deviated high-temperature, high-pressure exploration well in the North Sea. Offshore Technology Conference. OnePetro
Shen C (2015) Transient dynamics study on casing deformation resulted from lost circulation in low-pressure formation in the Yuanba Gasfield. Sichuan Basin Nat Gas Ind B 2(4):347–353
Wang P, Li H, Tan S, Huang X (2020) Multivariate global sensitivity analysis for casing string using neural network. Int J Comput Methods 17(05):1940015
Wang X, Qu Z, Dou Y, Ma W (2015) Loads of casing and cement sheath in the compressive viscoelastic salt rock. J Petrol Sci Eng 135:146–151
Wenkui L, Yanping X, Helin L, Zhihao J, Huilin G (1900) Effect of high-temperature and high-pressure on downhole casing strength. Oil Drill Prod Technol 27(3):15–17
Xie Y, Ouyang M, Zhao H, Li L, Feng Y (2021) Wellbore pressure management of offshore wells during casing running in narrow safety pressure window formations. J Petrol Sci Eng 199:108284
Yang L, Ming X, Yuqi F (2018) Causes of trapped annular pressure in high pressure gas wells in Central Sichuan and well cementing solution. Drill Fluid Complet Fluid 35(1):77–82
Yin Q et al (2022) Downhole quantitative evaluation of gas kick during deepwater drilling with deep learning using pilot-scale rig data. J Petrol Sci Eng 208:109136
Yin Y, Cai Y, Chen Z, Liu J (2006) Theoretical solution of casing loading in non-uniform ground stress field. Acta Petrolei Sinica 27(4):133–138
Zhang B et al (2018) Control and analysis of sustained casing pressure caused by cement sealed integrity failure. In: Offshore technology conference Asia. OnePetro
Zhang B et al (2022) Modeling and analysis of sustained annular pressure and gas accumulation caused by tubing integrity failure in the production process of deep natural gas wells. J Energy Resources Technol 144(6)
Zhang B et al (2021) Characteristics of sustained annular pressure and fluid distribution in high pressure and high temperature gas wells considering multiple leakage of tubing string. J Petrol Sci Eng 196:108083
Zhang Z et al (2020) The influence of hydrogen sulfide on internal pressure strength of carbon steel production casing in the gas well. J Petrol Sci Eng 191:107113
Zhao C, Li J, Zaman M, Jin Y, Tao Q (2021) Investigation of casing deformation characteristics under cycling loads and the effect on casing strength based on full-scale equipment. J Petrol Sci Eng 205:108973
Zhong L (2016) Status and prospect of key drilling and completion technologies for the development of HTHP gasfield in South China Sea. Oil Drill Prod Technol 38(6):730–736
Zhu X, Liu B (2018) The reliability-based evaluation of casing collapsing strength and its application in marine gas reservoirs. Eng Fail Anal 85:1–13

Authors and Affiliations

Chao Han[1,2] · Rongdong Dai[1] · Wenxue Pu[3] · Zhichuan Guan[4] · QiZhong Tian[1] · Haibin Zhao[3] · Xianming Ma[4] · Shengnan (Nancy) Chen[5] · Bo Zhang[6] · Chenglong Li[1,2] · Hui Shao[3] · Cong Zhang[3]

✉ Chao Han
hansuper713@hotmail.com

✉ Wenxue Pu
15692342210@163.com

[1] Petroleum Engineering Technology Research Institute of Shengli Oilfield, SINOPEC, Dongying, China

[2] Postdoctoral Scientific Research Working Station of Shengli Oilfield, SINOPEC, Dongying, China

[3] Geosteering and Logging Research Institute, Sinopec Matrix Corporation, Qingdao, China

[4] School of Petroleum Engineering, China University of Petroleum (East China), Qingdao, China

[5] Department of Chemical and Petroleum Engineering, University of Calgary, Calgary, Canada

[6] CNPC Research Institute of Safety and Environment Technology, Beijing, China